 doi:10.20944/preprints201911.0046.v1

Comparison among different fiber coatings on the concrete shrinkage test for distributed optical strain measurements based on Rayleigh backscattering

Martin Weisbrich*† Klaus Holschemacher† Thomas Bier‡

November 4, 2019

The fiber optic strain measurement based on Rayleigh scattering has recently become increasingly popular in automotive or mechanical engineering for strain monitoring and in the construction industry in general, especially structural health monitoring. This technology enables the monitoring of strain along the entire fiber length. Several publications have been published, particularly on the applications to the structural component. This article addresses integrating optical fibers of different coatings into the concrete matrix to measure the shrinkage deformations. In this context, three different coating types were investigated regarding their strain transfer. The fibers were integrated into fine-grained concrete prisms, and the shrinkage strain was compared with a precise dial gauge. The analysis shows a high correlation between the reference method and the fiber measurement, especially with the ORMOCER® coating. The used acrylate coating is also consistent in the middle area of the specimen but requires a certain strain introduction length to indicate the actual strain. The main result of this study is a recommendation for fiber coatings for shrinkage measurement in fine grain concretes using the distributed fiber

*Corresponding author, email: martin.weisbrich@htwk-leipzig.de
†Structural Concrete Institute, Leipzig University of Applied Science (HTWK Leipzig), Leipzig, 04275, Germany
‡Institute of Ceramics, Glass and Construction Materials, Technical University Freiberg, Freiberg, 09599, Germany

 doi:10.20944/preprints201911.0046.v1

optic strain measurement. In addition, the advantages and disadvantages of the measurement method are presented.

1 Introduction

The development of fiber optic sensors (FOS), especially distributed measurement methods, has led to interesting application scenarios in recent years [5, 17, 25, 28]. In particular, research groups published various applications for structural health monitoring (SHM) in civil engineering [2, 18, 23]. The measurement methods based on Rayleigh, Brillouin and Raman scatterings are suitable for the measurement tasks in SHM because of their distributed measurement principle. While Raman scattering only measures temperatures, Brillouin and Rayleigh scatterings can measure the temperature and strain [23]. The difference between these two methods can be found in the spatial resolution, maximum measuring length and the accuracy. Using Brillouin scattering, measurement tasks of several kilometers can be realized with a spatial resolution in the meter range [19, 25]. Rayleigh scattering has a maximum measuring length of approximately 70 m and a spatial resolution of a few millimeters [26].

The fiber optic strain measurement offers essential benefits compared to established measurement methods such as fiber Bragg grating sensors (FBG), strain gauges or inductive displacement transducers. In addition to their corrosion resistance, they are dielectric and immune to electromagnetic radiation [26]. Any point of the entire glass fiber can be used as the measuring range for the strain measurement and is not restricted to a pre-defined section [32]. Another advantage is the possibility of integrating the fiber into the building material matrix, which enables one to determine strain within concrete components, which can contain information on the curing and load behavior. Especially with massive concrete structures such as foundations or concrete roads, a strain measurement in the matrix can represent the structural and loading condition. In prefabricated elements, the quality management of posttreatment and health monitoring can be combined. However, information on the deformation within the matrix can also lead to new design approaches in the shrinkage, creep or swelling behavior of concrete components in research.

For a realistic representation of the strain in the matrix using fiber optic sensors, the investigation of the strain transfer from the substrate to the fiber is an elementary factor (Fig. 1 b). The strain is determined only in the fiber core (Fig. 1 a). Two mechanisms that have a decisive effect on the deformations of the fiber sensors: First, slippage can occur between the fiber cladding, so-called coating, and surrounding substrate. Second, depending on the coating material, the cladding cannot completely transfer the strain from the substrate to the fiber cladding and the core. The model by Cheng et al. was modified in this respect and is shown in Figure 1 b [4]. The slip relationship between the substrate and the fiber coating largely depends on the curing state of the concrete. Only when the concrete has sufficiently hardened can the strain transfer occur. The bond between coating material and concrete is critical for

Preprints (www.preprints.org) | NOT PEER-REVIEWED | Posted: 6 November 2019 doi:10.20944/preprints201911.0046.v1

the strain transfer. For the slip between the fiber coating and the fiber cladding, the stiffness of the coating material is decisive for adequate transfer [3, 30, 31].

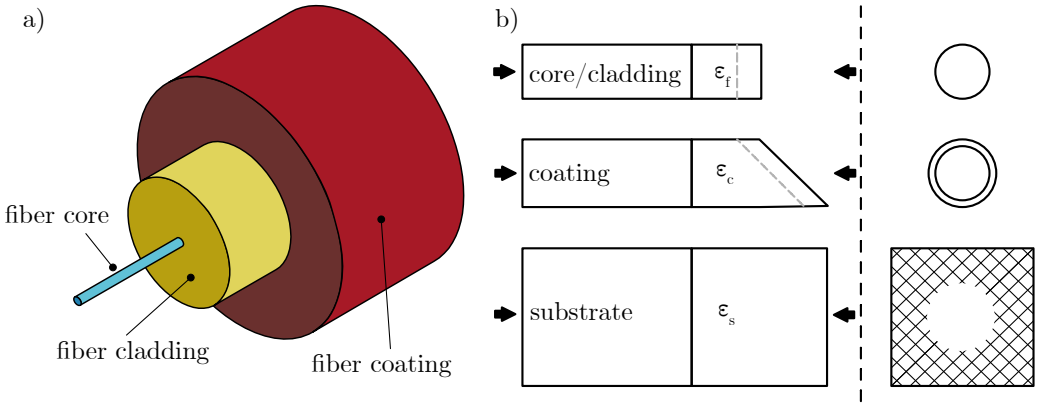

Figure 1: a) Structure of a fiber; b) Slip relationship between the matrix and the fiber core based on [4]

Various research groups have analyzed the effect of the fiber coating on the strain transfer during measurements in the matrix. For example, using Brillouin scattering, Zeng et al., could determine with the help of Brillouin scattering that fiber cables showed lower strain values in the matrix than the reference method [33]. Li Quingin et al. investigated the strain transfer rates of embedded FBG sensors in mortar prisms [22]. Using a calculation model, the group transferred the lower strain transfer rates (approx. 0.7-0.85) of a coating material to the reference measurement level. In 2003, the research group extended its model to include pressure loads [21]. Delephine-Lesoille et al. validated a specially developed fiber cable and integrated it into concrete cylinders subjected to compression and tension [6]. Thus, they achieved transfer rates of almost 100% in the range up to approximately $-350\,\mu\varepsilon$. Henault et al. also used fiber cables in 2010 to measure the strain in the concrete matrix [14]. In 2012, the research group investigated another type of cable [13]. Compared to the reference measurement, the sensors showed an approximately 20% lower strain value, so a calculation model for adjustment followed [15]. Regarding fiber cables, Bao et al. assumed that the strain sensitivity was too low [1]. In 2009, Li et al. examined various strain transfer models for different materials and confirmed them by experiments with sensors bonded to the surfaces [20]. For concrete with a modulus of elasticity of 40000 $\mathrm{N\,mm^{-2}}$, the researchers determined transfer rates of approximately 90%. Using a test program and an FE analysis, Her et al. established a transfer function, with which the raw data can be converted into the real strain [16]. Ohno et al. integrated fiber optic sensors into the compression and tensile zones of a concrete slab and checked the displayed strains [24]. They found that the fiber could not sufficiently anchor in the concrete structure. Using a brass frame, researchers fixed a fiber around Speck in small-format concrete specimens and achieved similar values to the reference measurement [27]. Fischer et al. compared fiber cables and two different coating materials for crack detection in

Preprints (www.preprints.org) | NOT PEER-REVIEWED | Posted: 6 November 2019 doi:10.20944/preprints201911.0046.v1

the matrix [10].

In summary, the presented publications do not adequately illustrate the effect of the coating on the strain transfer. In some cases, the specification of the coating used was completely omitted. Furthermore, in some investigations, the strain losses at lower loads are considerably higher than those in the tests. Therefore, the present study compares the effect of different coating materials on the strain measurement of the distributed fiber optic sensors (DFOS) in the concrete matrix. Thus, the strain transfer of three different coatings was investigated using shrinkage tests on fine-grained concrete prisms.

2 Experimental program

2.1 Coating materials and concrete mixture

The strain transfer properties of three different coating materials were investigated by using shrinkage tests. With two conventional coatings acrylate and polyimide, the results from the literature should be verified and form a baseline for comparison [10, 16, 22, 27]. The third coating material ORMOCER® was developed especially for FBG sensors and showed good strain transfer properties in previous investigations with bonded sensors [9, 31]. Table 1 summarizes the fiber types and their most important characteristics.

Table 1: Coating materials and fiber specifications

Coating material	Acrylate	Polyimide	ORMOCER®
Fibertype	SMF-28e+®	FSG-A01	LAL-1550-125
∅ Coating [µm]	242±5	155±5	195
∅ Cladding [µm]	125±0.7	125	125±1
Attenuation [dB km^{-1}]	< 0.02	< 0.6	< 2.5
Manufacturer	CORNING®	FBGS	FBGS

The matrix was a high-strength concrete with a maximum grain size of 2 mm. DYCKERHOFF cement was provided as a compound [8]; all other components are listed in Table 2. The fine-grained concrete was selected according to its high shrinkage tendency, which results in a correspondingly high load on the fiber.

2.2 Specimens and preparation

Concrete prisms with dimensions of b/h/l of 40 mm, 40 mm and 160 mm were used as the test specimen geometry. Three test specimens were produced per fiber type, which results in a test matrix of nine test specimens (Tab. 3). To integrate the fiber into the matrix, a modified formwork was used (Fig. 2 a), where the sensors were clamped and

Preprints (www.preprints.org) | NOT PEER-REVIEWED | Posted: 6 November 2019 doi:10.20944/preprints201911.0046.v1

Table 2: Concrete mixture for the shrinkage tests based on [8]

Matrix	Unit	Quantity
BMK-D5-1 (Compound)		815
BCS 0.06/0.2		340
Sand 0/2	[kg m^{-3}]	965
Water		190
Superplasticizer (MC-VP-16-0205-02)		17

cleaned with isopropanol. Immediately after concreting, the fiber was additionally tensioned to ensure the correct position in the specimen. A Teflon tube was used to minimize the risk of fiber breakage in the outlet areas and protruded 10 mm into the concrete matrix on each end-face (Fig. 2). The area protected by the tube was not included in the analysis and is marked accordingly in Figures 5 and 6.

Table 3: Specimen assignment and coating material for the shrinkage tests

Nr.	Assignment	Coating material	l_0 in [mm]
1	A-1-t_i		160,0
2	A-2-t_i	Acrylate	160,1
3	A-3-t_i		160,0
4	P-1-t_i		159,9
5	P-2-t_i	Polyimide	159,9
6	P-3-t_i		160,2
7	O-1-t_i		159,9
8	O-2-t_i	ORMOCER®	160,0
9	O-3-t_i		160,4

For the reference measurement method, special measuring pins must be glued in the middle of the end-faces (Fig. 4). In this regard, the fiber was arranged by an offset dimension of $e = 7$ mm. The null length l_0, which is required to determine the reference strain, corresponds to the specimen length. Table 3 summarizes the zero length, specimen designation, and associated coating materials.

2.3 Test arrangement and procedure

The test setup and procedure are based on the German standard DIN 52450 and are shown in Figure 3 [7]. At 24 hours after concreting, the test specimens were prepared for the strain measurement, which proceeded as follows:

- Stripping the test specimens

Preprints (www.preprints.org) | NOT PEER-REVIEWED | Posted: 6 November 2019 doi:10.20944/preprints201911.0046.v1

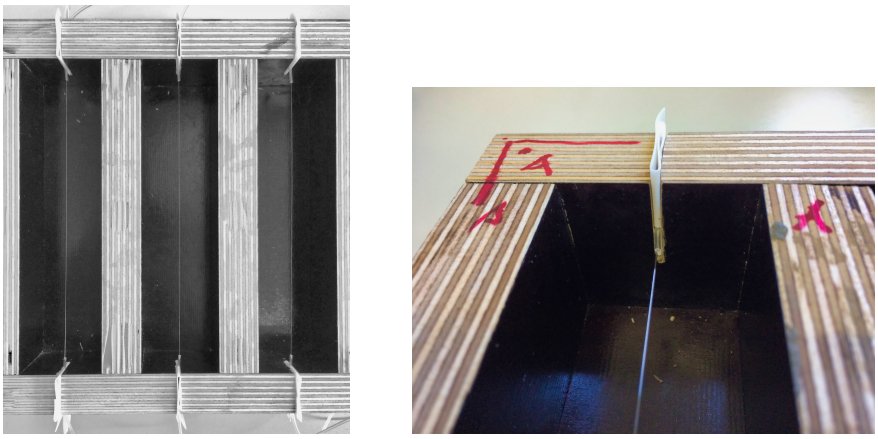

(a) (b)

Figure 2: a) Test specimen formwork with tensioned fiber; b) Fixed fiber with Teflon tube

- Applying the measuring pins and determining the null length l_0
- Clamping the specimens in the measuring frame (Fig. 4 b)
- Reading the reference value t_0 for both measuring methods

Table 4: Test times of the shrinkage tests

Time of measurement	Time after concreting [h]	[d]
t_0	24 ±1	1
t_1	96 ±1	4
t_2	192 ±1	8

During the experiment, the specimens were stored in a climatic box with constant climatic conditions (39% RH, 22 °C). Due to the relatively low humidity, the shrinkage load should be increased. The strain was measured using both measuring methods after 4 or 8 days after concreting. The measurement times are listed in Table 4.

2.4 DOFS system and reference measurement

The strain measurement of the fiber sensors performed with the interrogator ODiSi-B from Luna Inc. The interrogator measures the Rayleigh backscattering and uses coherent frequency domain reflectometry to determine the location of the strain along the fiber. Through the frequency shift between the unloaded reference state and the loaded state and a subsequent fast Fourier transformation (FFT), the deformations

Preprints (www.preprints.org) | NOT PEER-REVIEWED | Posted: 6 November 2019 doi:10.20944/preprints201911.0046.v1

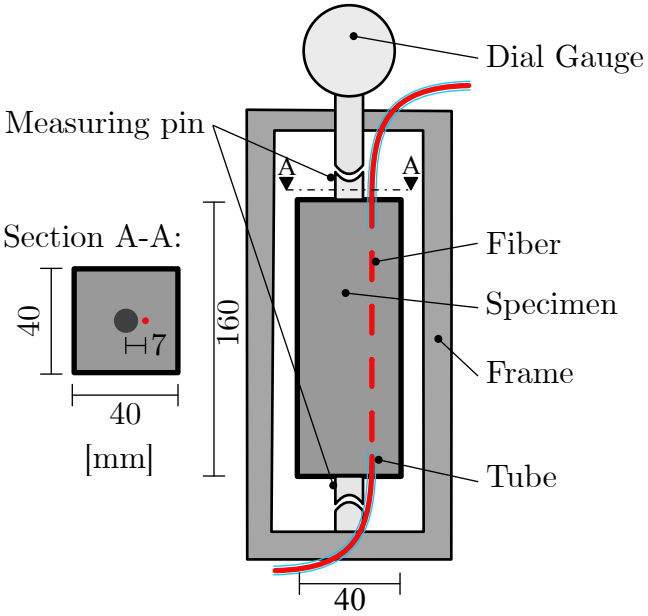

Figure 3: Arrangement of the test specimen and test setup

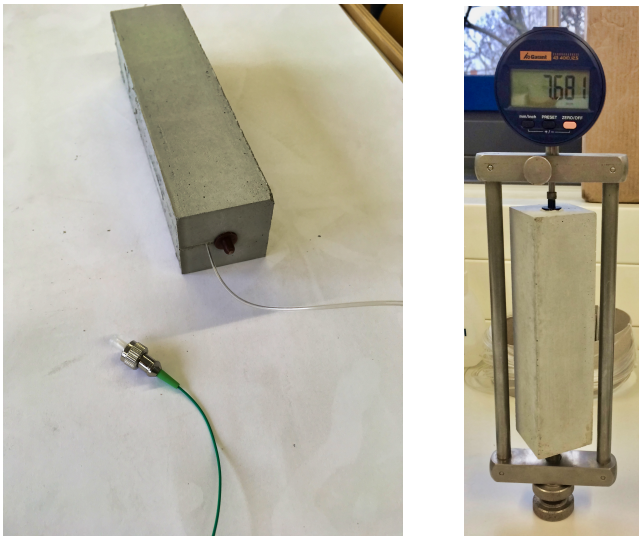

(a) (b)

Figure 4: a) Test specimen with sensor fiber and measuring pin; b) Test specimen in the measuring frame

Preprints (www.preprints.org) | NOT PEER-REVIEWED | Posted: 6 November 2019 doi:10.20944/preprints201911.0046.v1

can be determined. Further information on the measurement procedure can be found in the literature [11, 12, 26, 32].

Sensitive digital dial gauges were used as a reference method to measure the length change between the two measuring pins (Figures 3 and 4). The display of the difference is approximately 1/1000 mm; the error limit is 0.0005 mm.

2.5 Evaluation process

The fiber optic measurement method with its distributed measurement generates a considerable amount of data [31]: The method records a strain value for every 2.56 mm of the measuring fiber. To minimize the effect of the measurement noise, the strain values were recorded at a measuring rate of 1 Hz for 30 s at each measurement time t_i (Tab. 4).

A PYTHON-based postprocess was programmed to prepare the measurement raw data accordingly. As the first step, the relevant measuring range is delimited, which results in matrix X with approximately 62×30 measured values per sample and time of measurement.

$$X_{i,t_i} = \begin{pmatrix} \varepsilon_{t_{i,1,1}} & \cdots & \varepsilon_{t_{i,1,n}} \\ \vdots & \ddots & \vdots \\ \varepsilon_{t_{i,n,1}} & \cdots & \varepsilon_{t_{i,n,n}} \end{pmatrix} \tag{1}$$

System-related measurement errors are filtered by Akima interpolation [29]. Thus, the authors achieved better approximations than other interpolation or filter methods.

To reduce the measurement noise and improve the comparability with the reference method, the matrix of equation 1 is combined using a median to form a vector with the strain values:

$$\widetilde{x_{i,t_i}} = \left[\widetilde{\varepsilon_{t_{i,1}}} \cdots \widetilde{\varepsilon_{t_{i,n}}}\right] \tag{2}$$

Figures 5 and 6 show the individual vectors of the respective specimens. Then, the average strain values and standard deviation in the comparison range can be calculated. The results of the comparison range averaging are shown in Table 5; the mean values of the specimens are shown in Table 6.

3 Results

The main purpose of the experiments was to investigate the distributed fiber optic measurement method regarding the strain measurement in the concrete matrix. To this end, the shrinkage behavior of nine test specimens with different coating materials was investigated.

An overview of the results of the experiments is shown in Table 5. It contains the mean strain values of the fiber measurement in the comparison range, their associated

Preprints (www.preprints.org) | NOT PEER-REVIEWED | Posted: 6 November 2019 doi:10.20944/preprints201911.0046.v1

standard deviation along the fiber and the respective reference measurement at time points t_1 and t_2. The strain of the reference measurement results from the reference length l_0 (cf. Tab. 3) and measured value:

$$\varepsilon_r = \frac{\Delta_l}{l_0} \tag{3}$$

Table 5: Strain values and standard deviation in the comparison area of the fiber measurement compared to the strain values of the reference measurement at test times t_1 und t_2 in [με]

		Fiber Measurement				Reference Measurement	
		Average strain		Standard deviation			
Coating	Nr.	t_1	t_2	t_1	t_2	t_1	t_2
Acrylate	1	-583	-682	15	11	-594	-737
	2	-552	-662	26	28	-606	-737
	3	-523	-628	20	22	-581	-725
Polyimide	1	-580	-677	17	18	-613	-750
	2	-600	-710	14	14	-594	-732
	3	-549	-652	7	9	-587	-730
ORMOCER®	1	-569	-682	20	19	-563	-707
	2	-585	-702	11	13	-588	-706
	3	-549	-662	23	25	-586	-723

The mean values of the three specimens per fiber coating are shown in Table 6, and those of the reference measurement are shown in Table 7. The comparison of the two measurement methods can be characterized by the quotient between fiber measurement ε_f and reference measurement ε_r:

$$q = \frac{\varepsilon_f}{\varepsilon_r} \tag{4}$$

Table 6: Average strain values and standard deviation in the comparison area at test times t_1 und t_2 in [με]

	Strain		Standard deviation	
Coating	t_1	t_2	t_1	t_2
Acrylate	-553	-657	20	21
Polyimide	-576	-680	13	14
ORMOCER®	-568	-682	18	19

Preprints (www.preprints.org) | NOT PEER-REVIEWED | Posted: 6 November 2019 doi:10.20944/preprints201911.0046.v1

Table 7: Average strain values of the reference measurement [με]

Coating	t_1	t_2
Acrylate	-594	-733
Polyimide	-598	-738
ORMOCER®	-579	-712

Table 8: Mean strain quotients in the comparison area at test times t_1 und t_2

Coating	t_1	t_2
Acrylate	0.93	0,90
Polyimide	0.96	0,92
ORMOCER®	0.98	0.96

Figures 5 and 6 show the course of the strain along the fiber for all specimens at t_1 and t_2. The x-axis represents the fiber position, while the y-axis illustrates the shrinkage strain. The comparison area where the fiber freely lies in the matrix is highlighted in gray. The 10 mm in the inlet and outlet area indicates the fiber segments where the fiber was protected from mechanical effects by a tube (Fig. 3).

The values illustrate the high correlation between the fiber measurement and the reference measurement. Especially with the fiber coating ORMOCER®, the shrinkage strain can be almost completely transferred along the entire measuring length, which indicates a nearly loss-free strain transfer. During the acrylate coating, strain transfer losses were observed in the inlet and outlet areas of the fiber (cf. Figs. 5 and 6); in the center of the specimen, the strain increases to the level of the other two coatings.

The comparison between two measurement times t_1 and t_2 shows strain losses for increasing shrinkage deformation. Although the strain transfer quotient (Tab. 8) of the acrylate and polyimide fibers decreases by $< 4\%$, the loss in ORMOCER® coating is constant at $< 2\%$.

In summary, the test design is well suited for assessing the shrinkage behavior with fiber-optic strain measurements. Furthermore, the usefulness of the DOFS for the measurement of deformations in the matrix of fine grain concretes is shown. All specimens were similarly produced and show minor artifacts (Fig. 5, O2). Basically, only the ORMOCER® coating shows indicates a loss-free strain transfer compared to the reference measurement and can be used for shrinkage measurement ($t_1 < 2\%$, $t_2 < 4\%$). In the acrylate coating, strain losses were observed in the inlet and outlet areas of the fiber in the specimen, and they indicate a slip between coating and cladding (cf. Fig. 1 b). The strains in the middle area of the specimen reached those of the other coating materials. In the case of polyimide and acrylate coatings, small losses ($< 3\%$) were observed between two measurement points during the strain transfer and losses of approximately 8-10% compared to the reference measurement.

Preprints (www.preprints.org) | NOT PEER-REVIEWED | Posted: 6 November 2019 doi:10.20944/preprints201911.0046.v1

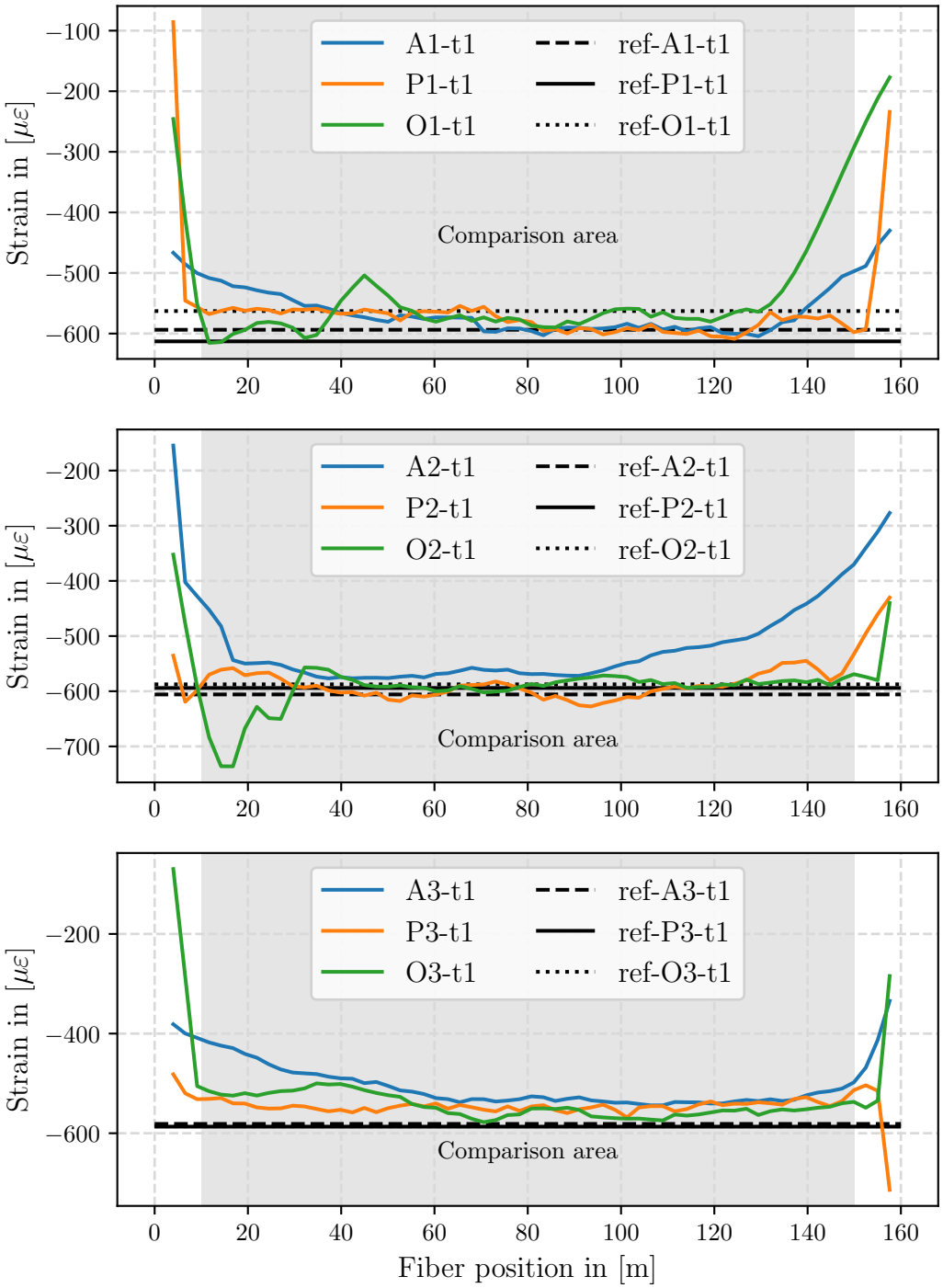

Figure 5: Strain profiles of all specimens at test time t_1

Preprints (www.preprints.org) | NOT PEER-REVIEWED | Posted: 6 November 2019 doi:10.20944/preprints201911.0046.v1

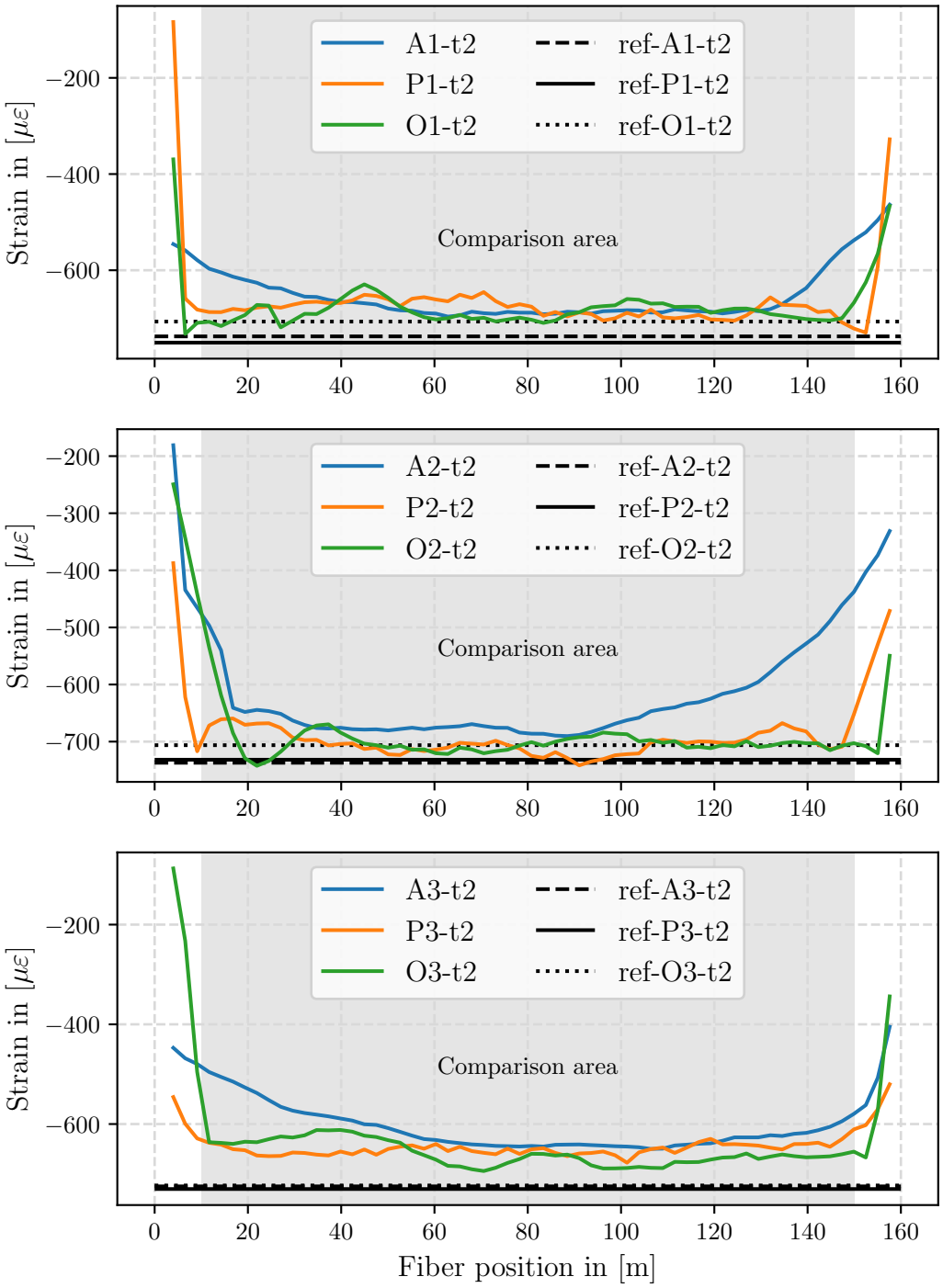

Figure 6: Strain profiles of all specimens at test time t_2

Preprints (www.preprints.org) | NOT PEER-REVIEWED | Posted: 6 November 2019 doi:10.20944/preprints201911.0046.v1

4 Discussion

The fiber optic sensor technology offers interesting advantages over the established measurement methods for strain measurement in the matrix. With the use of DOFS, the strain can be determined at every point of the fiber, and the sensor fiber can be directly integrated into the concrete structure. Particularly with massive concrete components, differences can occur in the shrinkage measurement at the surface compared to that in the matrix. For a strain measurement that corresponds to the real deformation of the component, the strain transfer between substrate and coating and between coating and cladding should be investigated (Fig. 1). Only the frequency shift in the fiber core can be used to determine the strain. In addition to the slip relationship, the correct integration of the fiber into the concrete structure is a challenge. The sensor must retain its intended position even after concreting. Another important aspect is the curing time of the fresh concrete. Only when the concrete has sufficiently hardened, the deformations can be transferred to the fiber. In the tests, measurement was started 24 hours after concreting.

Basically, the results show that the Ormocer® coating material can be used for an adequate strain measurement in fine grain concretes. In the case of polyimide coating, small losses of ¡8% were observed. Only for acrylate coating should a strain initiation length of at least 40 mm be provided. The lower stiffness of the material may cause poorer strain transfer in these areas. The acrylate and polyimide coatings showed low losses of $< 3\%$ at time t_2 compared to the measurement after three days. The bond between substrate and coating is assumed to cause the deficits. Except for the entrance area at sample O-2 (Tab. 3, Fig. 5), all specimens were close to each other and only slightly different from the reference measurement. Considering the imprecision of both measuring methods, the mentioned deviations are negligibly small.

The tests form a basis for the possibilities of the DOFS to measure the strain in the concrete matrix and the SHM of concrete components, especially for precast elements. In addition, the strain transfer properties of the three coating materials for deformation measurements in the matrix are evaluated in more details. However, further investigations are necessary for SHM: For example, the behavior of the fiber sensor remains unclear regarding the position when larger aggregates are used. Another important aspect is the protection of the fiber against destruction. The moisture, aggregates of the concrete and paving conditions on the construction site are important in this respect. Strain cables can help here. However, in contrast to fibers that are exclusively protected by the coating, the larger structure of cables increases the slip-related expansion losses. Furthermore, the long-term stability of the sensors is unclear. In particular, the moist, alkaline milieu of concrete can impair the expansion transfer during long-term monitoring. In addition to the investigation of other coating materials and cable types, the behavior of the fiber sensors under mechanical loads will be a future object of investigation. Until now, the measuring method has only been tested under pressure loads for the presented case. The strain transfer behavior under tensile loads and the resulting formation of cracks remain unclear.

Preprints (www.preprints.org) | NOT PEER-REVIEWED | Posted: 6 November 2019 doi:10.20944/preprints201911.0046.v1

5 Conclusion

The investigation compared different coating materials for their strain transfer properties during the strain measurement in the matrix using shrinkage tests. If the represented requirements are fulfilled, exact and reproducible results can be achieved with the ORMOCER® coating material. The following conclusions are drawn from the study:

- The exact position of the fiber in the matrix during and after concreting is decisive for the indicated strains.
- The concrete should be sufficiently cured to guarantee the strain transfer. In the tests, the measurement was begun after 24 hours.
- With the ORMOCER® coating, almost no strain losses were detected at the first sampling time.
- In the case of the acrylate and polyimide coatings, an approximately 3% loss occurred between the first and second measurements.
- The acrylate coating showed higher strain losses in the boundary areas than in the middle of the test specimen (max. 37%). From a strain introduction length of approximately 40 mm, the acrylate fiber showed strains at the level of the reference measurement and two other coating materials.
- For the immense amount of data, additional postprocesses and error algorithms are necessary to exclude system-related measurement errors and precisely display the results.

Data availability. The datasets used and analyzed in the current study are available from the corresponding author on reasonable request.

Author contributions. MW performed the experiments with the distributed optic sensors, evaluated the data in relation to the topic, and wrote the final paper. KH and TB accompanied the experiments and advised on the conceptual design of the paper. All authors read and approved the final paper.

Competing interests. The author declare that they have no conflict of interest.

Acknowledgments. This research is co-financed by tax revenues on the basis of the budget adopted by the members of the Saxon Parliament (promotion reference: K- 7531.20/434-14; SAB no. 100316843). Furthermore, WILEY AUTHOR SERVICES proofread the paper.

References

[1] Bao, X. and Chen, L. "Recent Progress in Distributed Fiber Optic Sensors". In: *Sensors* 12.7 (June 2012), pp. 8601–8639. DOI: 10.3390/s120708601.

[2] Barrias, A. et al. "Application of distributed optical fiber sensors for the health monitoring of two real structures in Barcelona". In: *Structure and Infrastructure Engineering* 14.7 (Feb. 2018), pp. 967–985. DOI: 10.1080/15732479.2018.1438479.

[3] Betz, D. C. et al. "Advanced layout of a fiber Bragg grating strain gauge rosette". In: *Journal of lightwave technology* 24.2 (2006), pp. 1019–1026.

[4] Cheng, C.-C. et al. "An investigation of bonding-layer characteristics of substrate-bonded fiber Bragg grating". In: *Journal of lightwave technology* 23.11 (2005), p. 3907.

[5] Czarske, J. and Müller, H. "Heterodyne detection technique using stimulated Brillouin scattering and a multimode laser". In: *Optics Letters* 19.19 (Oct. 1994), p. 1589. DOI: 10.1364/ol.19.001589.

[6] Delepine-Lesoille, S. et al. "Quasi-distributed optical fibre extensometers for continuous embedding into concrete: design and realization". In: *Smart Materials and Structures* 15.4 (May 2006), pp. 931–938. DOI: 10.1088/0964-1726/15/4/005.

[7] *DIN 52 450:1985-08, Testing of inorganic non-metallic building materials; Determination of shrinking and swelling on small test pieces.* (DIN 52450:1985).

[8] Dyckerhoff GmbH. *C3 Carbon Concrete Composite. Bindemittel für hochfeste Carbonbetone.* Feb. 1, 2017. URL: http://www.dyckerhoff.com/online/de/Home/Unternehmen/ForschungundEntwicklung/Projekte/documento423.html (visited on 09/17/2019).

[9] FBGS International N.V. *DTG coating Ormocer®-T for Temperature Sensing Applications.* Feb. 1, 2015. URL: https://fbgs.com/wp-content/uploads/2019/03/Introducing_and_evaluating_Ormocer-T_for_temperature_sensing_applications.pdf (visited on 09/16/2019).

[10] Fischer, O., Thoma, S., and Crepaz, S. "Quasikontinuierliche faseroptische Dehnungsmessung zur Rissdetektion in Betonkonstruktionen". In: *Beton- und Stahlbetonbau* 114.3 (Jan. 2019), pp. 150–159. DOI: 10.1002/best.201800089.

[11] Froggatt, M. and Moore, J. "High-spatial-resolution distributed strain measurement in optical fiber with Rayleigh scatter". In: *Applied Optics* 37.10 (1998), pp. 1735–1740.

[12] Gifford, D. K. et al. "Distributed fiber-optic temperature sensing using Rayleigh backscatter". In: *2005 31st European Conference on Optical Communication, ECOC 2005.* Vol. 3. IET. 2005, pp. 511–512.

[13] Henault, J.-M. et al. "Quantitative strain measurement and crack detection in RC structures using a truly distributed fiber optic sensing system". In: *Construction and Building Materials* 37 (Dec. 2012), pp. 916–923. DOI: 10.1016/j.conbuildmat.2012.05.029.

[14] Henault, J.-M. et al. "Truly Distributed Optical Fiber Sensors for Structural Health Monitoring: From the Telecommunication Optical Fiber Drawling Tower to Water Leakage Detection in Dikes and Concrete Structure Strain Monitoring". In: *Advances in Civil Engineering* 2010 (2010), pp. 1–13. DOI: 10.1155/2010/930796.

[15] Henault, J. et al. "Analysis of the strain transfer mechanism between a truly distributed optical fiber sensor and the surrounding medium". In: *Concrete Repair, Rehabilitation and Retrofitting III*. CRC Press, 2012, pp. 288–289.

[16] Her, S.-C. and Huang, C.-Y. "Effect of Coating on the Strain Transfer of Optical Fiber Sensors". In: *Sensors* 11.7 (July 2011), pp. 6926–6941. DOI: 10.3390/s110706926.

[17] Horiguchi, T. et al. "Development of a distributed sensing technique using Brillouin scattering". In: *Journal of Lightwave Technology* 13.7 (July 1995), pp. 1296–1302. DOI: 10.1109/50.400684.

[18] Inaudi, D. and Glisic, B. "Application of distributed fiber optic sensory for SHM". In: *Proceedings of the ISHMII-2* 1 (2005), pp. 163–169.

[19] Leung, C. K. Y. et al. "Review: optical fiber sensors for civil engineering applications". In: *Materials and Structures* 48.4 (Nov. 2013), pp. 871–906. DOI: 10.1617/s11527-013-0201-7.

[20] Li, H.-N. et al. "Strain Transfer Coefficient Analyses for Embedded Fiber Bragg Grating Sensors in Different Host Materials". In: *Journal of Engineering Mechanics* 135.12 (Dec. 2009), pp. 1343–1353. DOI: 10.1061/(asce)0733-9399(2009)135:12(1343).

[21] Li, Q., Li, G., and Wang, G. "Effect of the plastic coating on strain measurement of concrete by fiber optic sensor". In: *Measurement* 34.3 (Oct. 2003), pp. 215–227. DOI: 10.1016/s0263-2241(03)00052-6.

[22] Li, Q. et al. "Elasto-Plastic Bonding of Embedded Optical Fiber Sensors in Concrete". In: *Journal of Engineering Mechanics* 128.4 (Apr. 2002), pp. 471–478. DOI: 10.1061/(asce)0733-9399(2002)128:4(471).

[23] López-Higuera, J. M. et al. "Fiber optic sensors in structural health monitoring". In: *Journal of lightwave technology* 29.4 (2011), pp. 587–608.

[24] Ohno, H. et al. "Industrial Applications of the BOTDR Optical Fiber Strain Sensor". In: *Optical Fiber Technology* 7.1 (Jan. 2001), pp. 45–64. DOI: 10.1006/ofte.2000.0344.

[25] Parker, T. et al. “A fully distributed simultaneous strain and temperature sensor using spontaneous Brillouin backscatter”. In: *IEEE Photonics Technology Letters* 9.7 (July 1997), pp. 979–981. DOI: 10.1109/68.593372.

[26] Samiec, D. “Distributed fibre-optic temperature and strain measurement with extremely high spatial resolution”. In: *Photonic International* 6 (2012), pp. 10–13.

[27] Speck, K. et al. “Faseroptische Sensoren zur kontinuierlichen Dehnungsmessung im Beton”. In: *Beton- und Stahlbetonbau* 114.3 (Jan. 2019), pp. 160–167. DOI: 10.1002/best.201800105.

[28] Udd, E. *Fiber optic sensors: an introduction for engineers and scientists*. Wiley-Blackwell, Aug. 5, 2011. 512 pp. ISBN: 0470126841. URL: https://www.ebook.de/de/product/13230722/eric_udd_fiber_optic_sensors.html.

[29] Ueberhuber, C. W. *Numerical Computation 1*. Springer Berlin Heidelberg, Feb. 27, 1997. 496 pp. ISBN: 3540620583. URL: https://www.ebook.de/de/product/14678306/christoph_w_ueberhuber_numerical_computation_1.html.

[30] Wan, K. T., Leung, C. K., and Olson, N. G. “Investigation of the strain transfer for surface-attached optical fiber strain sensors”. In: *Smart Materials and Structures* 17.3 (2008), p. 035037.

[31] Weisbrich, M. and Holschemacher, K. “Comparison between different fiber coatings and adhesives on steel surfaces for distributed optical strain measurements based on Rayleigh backscattering”. In: *Journal of Sensors and Sensor Systems* 7.2 (Nov. 2018), pp. 601–608. DOI: 10.5194/jsss-7-601-2018.

[32] Weisbrich, M., Holschemacher, K., and Kaeseberg, S. “Comparison between different Fiber Optical Strain Measurement Systems Based on the Example of Reinforcing Bars”. In: *Procedia Engineering* 172 (2017), pp. 1235–1242. DOI: 10.1016/j.proeng.2017.02.145.

[33] Zeng, X. et al. “Strain measurement in a concrete beam by use of the Brillouin-scattering-based distributed fiber sensor with single-mode fibers embedded in glass fiber reinforced polymer rods and bonded to steel reinforcing bars”. In: *Applied Optics* 41.24 (Aug. 2002), p. 5105. DOI: 10.1364/ao.41.005105.